Letter

Temperature Dependence of X-ray-Induced Auger Processes in Liquid Water

Clara-Magdalena Saak, Isaak Unger, Geethanjali Gopakumar, Carl Caleman, and Olle Björneholm*

Read Online

ACCESS | Metrics & More | Article Recommendations

ABSTRACT: Auger spectroscopy has previously been used to study changes in the hydrogen bond network in liquid water, but to the best of our knowledge it has not been used to track such changes as a function of temperature. We show Auger spectroscopy to reflect the weakening of the hydrogen bond network upon heating. This shows that the radiation response of water, i.e., the relative propensity of the different processes occurring after radiation exposure, including femtosecond proton dynamics, depends on the temperature of the system. This proof-of-principle study further demonstrates the suitability of the technique to help elucidate information on the intermolecular structure of liquids such as water, opening the door to further temperature-dependent studies.
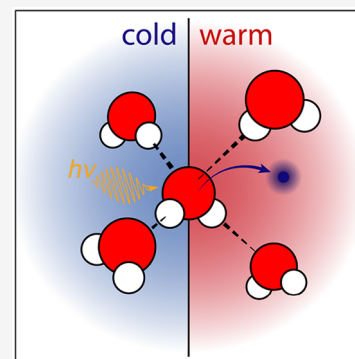
Auger electron spectroscopy is uniquely suited to investigate the local environment of molecules,[1−4] because it combines chemical selectivity (via core ionization) and sensitivity to the valence states that participate in any inter- and intramolecular interaction. In addition, Auger spectroscopy provides temporal information about processes occurring on the time scale of the core-hole lifetime, i.e., a few femtoseconds. The possible Auger decay processes in a condensed system can be conceptually separated into *local* decay occurring within the core-ionized molecule and *nonlocal* decay involving the electron density of neighboring molecules. For condensed water, the latter can be further divided into *interatomic Coulombic decay* (ICD)[2,5−7] and *electron transfer mediated decay* (ETMD),[8,9] which occur in the ground-state geometry, and *proton transfer mediated charge separation* (PTM-CS), which involves proton dynamics in the core-ionized state and was first observed in pure water.[10] In principle, the different decay channels that contribute to the total Auger spectrum (local, nonlocal, and excited-state nuclear dynamics) each contain information about different aspects of the intermolecular structure. The ratio of local/nonlocal decay depends on the distance and number of the nearest-neighbor molecules. The dynamics of protons in the excited state, on the other hand, have been linked to hydrogen bonding in the ground state.

We have previously used this technique to study the intermolecular network of liquid methanol.[11] To the best of our knowledge, however, it has not been investigated whether a change in temperature, which subtly changes the liquid structure, influences the relative propensity of the different Auger channels (local and nonlocal) and the PTM-CS process.

No significant temperature effects on Auger decay of the free molecule is expected, because kT is still too low to excite states beyond low-energy rotational modes.

Here, we present the first temperature-dependent O 1s Auger spectra of liquid water. We find the different decay channels contributing to the total Auger spectrum are sensitive to the changes in local structure which accompany heating of the liquid. Because the structure of liquid water at different temperatures has been studied in detail, we know that any changes we observe can be attributed to changes in the strength of the water–water interactions. Through our experiments, we are indeed able to observe the expected weakening of the hydrogen bond network of water as the temperature is raised (i.e., decreasing hydrogen bonding with increased temperature). We also observe the decreased density of liquid water at higher temperature, as reflected in the decreased propensity for nonlocal decay in the O 1s Auger spectrum obtained at higher temperature. Our work shows that the radiation response of water, i.e., the relative propensity of the different processes occurring after radiation exposure, depends on the temperature of the system.

In the Auger decay of the O 1s core vacancy, a valence electron of the same molecule fills the O $1s^{-1}$ core hole and the
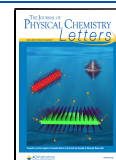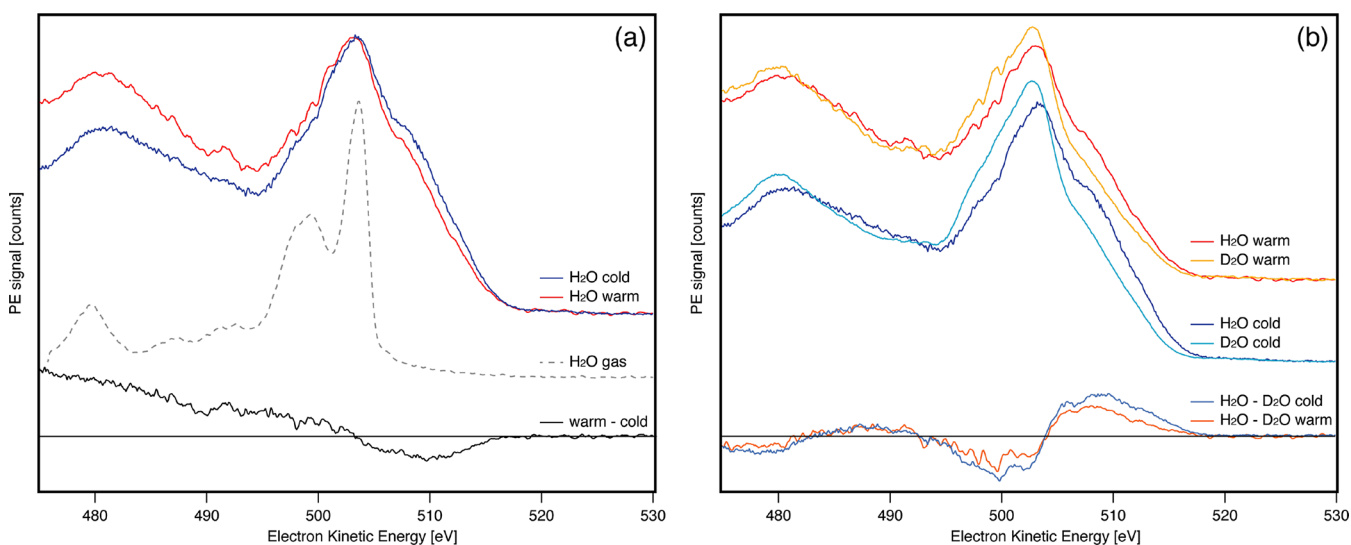
Figure 1. Comparison of O 1s Auger spectra of cold and warm water: (a) nonlocal versus local and (b) isotope effect. The gas-phase spectrum has been shifted in kinetic energy to align its main peak with that of the liquid traces.

excess energy is dissipated by the emission of a secondary electron from a valence state. This decay mechanism is referred to as *local decay* throughout the text. When the density of molecules around the ionization site is sufficiently high, the decay process can also involve the electronic states of these neighboring molecules via ICD[2,5−7] and ETMD.[8,9] Both of these decay channels lead to a final state in which the total charge (2+) is distributed over two molecules, which leads to a lower energy of the final states and hence higher kinetic energy (KE) of the secondary electron, compared with the local decay channel.

During the lifetime of the intermediate O $1s^{-1}$ excited state, approximately 4 fs,[12] some nuclear relaxation can occur before the electronic decay into the final state. Such nuclear dynamics occurring in the core-ionized excited state have been described in previous publications[13−15] under the term *ultrafast dissociation*. In the case of liquid water, proton transfer during the lifetime of the O $1s^{-1}$ intermediate state has been studied in detail by Thürmer et al.[10] The water O $1s^{-1}$ state is not dissociative in the gas phase, but dissociation becomes allowed in the hydrogen-bonded condensed phase. The decay process involving such proton dynamics has been termed *proton transfer mediated charge separation* (PTM-CS)[10,16] in water, because the loss of the proton decreases the total charge on the ionized molecule. The charge separation lowers the energy of the final state, which can be observed spectroscopically as an increase in kinetic energy of the secondary electron.

In order to separate the PTM-CS feature from other nonlocal decay channels, deuterium is substituted for hydrogen in the sample. The higher mass of the isotope leads to decreased dispersion of the wave packet in the excited state; that is, a higher percentage of states decay close to the ground-state geometry.[10] All other nonlocal processes are largely unaffected by the isotopic substitution, as the geometric and electronic structure of the system is not significantly altered by the isotopic substitution.

To study the effect of proton dynamics and charge separation on the postionization processes in liquid water of different temperature, a series of Auger O 1s spectra were recorded for liquid water alongside its deuterated equivalent. The gas-phase contribution to each spectrum was subtracted

from the Auger traces, yielding the "liquid-only" traces, which were then normalized to their total area. The liquid-only traces of water and heavy water are then subtracted from one another ($H_2O − D_2O$), in order to produce a difference spectrum (total area = 0) showing the relative redistribution of signal intensity from low to high kinetic energy due to proton dynamics.

Because of the ill-defined temperature of the liquid jet in vacuum, experiments were performed at two temperatures only, which are defined by the temperature of the water bath (T_{set} = 5 and 80 °C) that is used to equilibrate the temperature of the sample before the liquid jet is formed and are termed simply "cold" and "warm" throughout the text. This set temperature defines the upper limit of the temperature of the liquid jet, before its temperature drops because of evaporative cooling in the vacuum of the experimental chamber. The cooling of a liquid jet's bulk temperature has been studied using Raman spectroscopy by Wilson et al.[17] in the case of a room-temperature liquid jet. On the basis of this work and our experimental geometry, we estimate that the bulk temperature is lowered by approximately 15 °C. However, the cooling rate of the cold jet (T_{set} = 5 °C) is likely lower because of the decreased vapor pressure and in turn higher in the case of the heated liquid (T_{set} = 80 °C). We therefore estimate the temperature of the bulk liquid to be in the range of 10 to −5 °C, and 80 to 60 °C at the point of ionization.

The Auger spectrum of water vapor is shown in Figure 1. This spectrum consists of transitions from the O $1s^{-1}$ intermediate state to a multitude of final states with two valence holes. The Auger spectrum of water in different phases has previously been described in the literature in detail.[1,2,10] As previously discussed and reported, the highest-energy Auger electrons result from transitions involving the outer-valence states of the molecule, such as the nonbonding lone pairs of the oxygen site. Transitions involving the inner-valence states then appear at progressively lower kinetic energy. The gas-phase O 1s Auger spectrum has a prominent main feature at ∼500 eV. At lower kinetic energy (<500 eV), a progression of smaller peaks is found. The O 1s Auger spectra of the liquid target contain significant contributions from the gas phase of evaporating molecules surrounding the liquid jet. The gas-
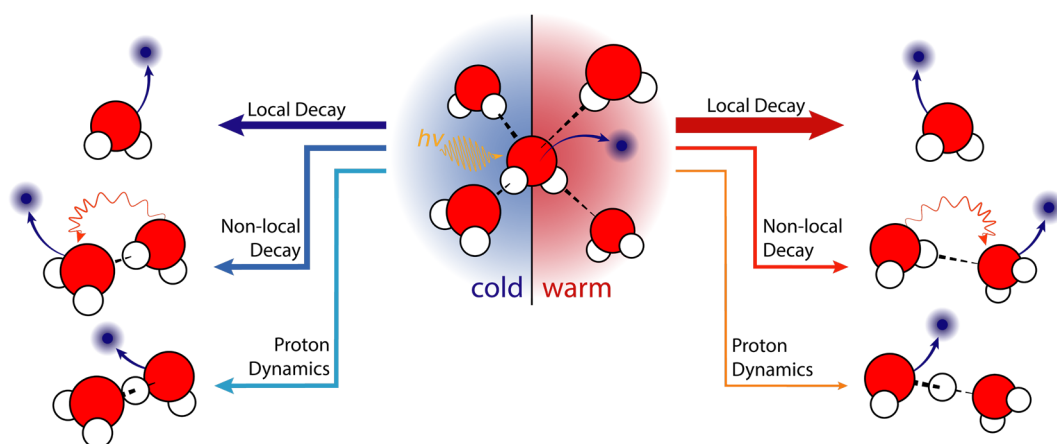
Figure 2. Sketch showing the relative propensities of local Auger, nonlocal Auger, and proton-transfer dynamics in cold (left) and warm (right) water. While the same relaxation channels are open at both temperatures, their relative propensity is affected. The thickness of the arrow indicating the different decay processes qualitatively represents the relative propensity of the respective decay channels. As the temperature increases, processes involving a neighboring molecule are found to be less likely, largely because of the decreased density of the liquid and the weakening of the hydrogen bond network.

phase subtracted liquid-only traces of water and heavy water in the cold and warm system are displayed in Figure 1. The liquid-only O 1s Auger spectrum is composed of two overlapping peaks at 504 and 509.5 eV kinetic energy. The lower kinetic energy region of the spectrum (<495 eV) features a series of overlapping broad peaks.

The local/molecular Auger decay channels in the liquid-phase spectra are equivalent to the transitions found in the gas phase, but the peaks are broadened and shifted to lower kinetic energies. The shift can simply be attributed to the added screening of the charges in both the intermediate core-ionized state and doubly valence ionized final state that takes place in the condensed phase. The broadening effect is due to variations in the polarization screening due to a distribution of local geometries around the ionized site in the liquid phase and any additional low-energy intermolecular vibrations. These effects of polarization screening on the Auger spectrum have been outlined in detail for water clusters by Öhrwall et al.[2]

Any peaks in the liquid phase spectrum that cannot be assigned to a corresponding gas-phase peak are attributed to decay channels involving the neighboring molecules of the ionization site. These nonlocal decay channels lead to a final state in which the double vacancy is shared between two molecules, which is lower in energy than the final state of local decay. This in turn increases the kinetic energy of the secondary electron that is produced as a product of nonlocal decay. From the comparison shown in Figure 1 it becomes apparent that these channels significantly contribute to the decay processes of the O $1s^{-1}$ state in water, by forming a shoulder around 510 eV that is absent in the gas-phase spectrum. The contributions from nonlocal channels we observe in this shoulder are the ones with a sufficiently high kinetic energy such that they appear in a region where there is no contribution from the local decay. There may well be, however, more nonlocal transitions that merge with the continuum of transitions at lower kinetic energy. What we observe and discuss here is thus a lower limit to how much nonlocal transitions contribute to the total O 1s decay in the system. To compare the propensity for nonlocal decay in cold and warm water, the two spectra are normalized to the intensity of the main peak and subtracted from one another (warm − cold); both spectra and the resulting difference trace

is shown in Figure 1a. As can be seen by the negative area of the difference trace around 510 eV kinetic energy, the relative propensity for nonlocal decay is considerably decreased when the system is heated, namely by a loss of relative signal intensity by a factor of approximately 0.9. The positive contribution to the difference trace at kinetic energies less than 505 eV corresponds to the increased scattering of electrons in the warm system by the more dense water vapor surrounding the liquid jet. The warm traces show a noise contribution on the lower kinetic energy flank of the main peak (~495−505 eV), which is due to imperfect gas-phase subtraction; however, the error introduced by the incomplete gas-phase subtraction does not affect the results presented below.

During the lifetime of the intermediate O $1s^{-1}$ core hole state (4 fs[12]) both local and nonlocal decay channels can occur in parallel with nuclear dynamics in the $1s^{-1}$ state.[16,18] As previously outlined, any dynamic processes involving nuclear motion that occur in the intermediate core hole state happen on a slightly different time scale depending on whether the system contains hydrogen (H) or deuterium (D). A redistribution of the relative signal intensity in the Auger region due to isotopic substitution, i.e., the isotope effect, is therefore an indication that such processes take place in the system. Figure 1b shows the comparison between the liquid-only spectra of water and its deuterated equivalent at both the cold and the warm temperatures. In both cases, there is an appreciable isotope effect in the O 1s Auger region, as previously reported for cold water by Thürmer et al.,[10] i.e., a relative increase of intensity on the high kinetic energy flank of the H_2O spectrum compared with D_2O. This redistribution of relative signal intensity can be attributed to proton-transfer dynamics occurring at the oxygen site during the lifetime of the intermediate O $1s^{-1}$ state. The isotope effect is less pronounced in the case of warm water than cold water, as can be seen in the relative area of the difference traces, displayed in Figure 1b. From the difference traces it can be seen that the general shape of the isotope effect (mainly a reduced relative intensity between ~493−504 eV and a relative signal increase between ~504−518 eV) is maintained at the higher temperature; however, the magnitude of the effect is reduced by a factor of approximately 0.7. We attribute this change in the relative isotope effect to the well-known change

in the hydrogen-bonding network at increased temperature. Other changes to the liquid's properties may also contribute to the observed temperature effect, such as the reduced influence of nuclear quantum effects at higher temperatures; however, the contribution from such effects is likely small compared with the reduced hydrogen bond strength. It is currently not possible to estimate the relative impact of all contributions, and we focus our discussion on the dominant influence of hydrogen bonding itself.

The changes to water's structure due to temperature have been investigated in a number of publications, with the most relevant changes for our work being the interconnected properties of the decrease in average density[19] and the corresponding increase in nearest-neighbor distance,[20] as well as the weakening of the intermolecular hydrogen bond network. The latter can be seen both in the previously mentioned increased nearest-neighbor distance but also in the decreasing number of hydrogen bonds per molecule,[21] as well as a loss of molecular alignment along the hydrogen bond axis[22] of the liquid with increasing temperature.

The changes to the Auger spectrum at higher sample temperature can be explained by these reported changes to the intermolecular structure of water. First, the increased temperature decreases the density of the bulk liquid, which reduces the nonlocal decay propensity, as it is related to the distance between the two molecular units. The weakened isotope effect at higher temperature can be attributed to weakening of the hydrogen bond network.

We can clearly observe temperature-induced structural changes in the system reflected in the O 1s Auger spectrum, both in terms of the average intermolecular distances and the changes in the strength of the hydrogen-bonding network. The changes to the relative propensity of the different decay channels (local Auger, nonlocal Auger, and PTM-CS) are qualitatively summarized in Figure 2. This shows that the radiation response of liquid water is affected by temperature, and the propensity for the different decay channels is highly sensitive to the local structure of the system.

In conclusion, we have presented data that show the O 1s Auger spectrum of liquid water to be sensitive to changes in the system's temperature. This sensitivity comes about because of subtle changes in the intermolecular structure, such as the density and strength of the hydrogen bond network, to which the different channels contributing to the Auger decay spectrum are sensitive. These changes affect both the branching ratio between local and nonlocal decay, as well as the efficiency of the PTM-CS process. In the case of the nonlocal/local decay, the decrease in the relative propensity for nonlocal decay upon heating indicates a loss of molecular density around the ionization site, as expected. Similarly, the decreased isotope effect describes the weakening hydrogen bonding network at higher temperatures. While these changes to the water structure with temperature are well-known, it is important to note that the Auger decay spectrum is sensitive enough to reflect them, opening the possibility of using this technique to study the local structure of liquids under different conditions, where the effects on hydrogen bonding are less well-known.

■ EXPERIMENTAL SECTION

Experiments were performed at the SOL^3 endstation[23] located at the U49-2/PGM1 beamline[24] of the BESSYII storage ring at Helmholtz-Zentrum Berlin. The target was a 25 μm diameter liquid jet, which was perpendicularly intersected with linearly polarized soft X-ray radiation. The hemispherical electron analyzer was mounted at the magic angle ($\sim$55°) relative to the horizontal polarization of the synchrotron radiation. The XPS measurements of the valence states, O 1s core level, and O 1s Auger region were obtained with a photon energy of 600 eV. Gas-phase spectra were recorded by disaligning the liquid jet and measuring on the evaporating vapor.

In order to avoid charging of the sample because of insufficient conductivity of the liquid, 50 mM NaCl (Sigma-Aldrich, >99.8% purity) was added to both the H_2O and D_2O samples.

The kinetic/binding energy scale for the spectra was calibrated on the lowest binding energy valence peak of the liquid. The binding energy of the H_2O $1b_1$ peak was previously reported to be 11.16 eV.[25] This accounts for any potential offset in the photon energy and effects of the streaming potential,[26] which have been observed to significantly alter the apparent binding energy in the case of liquid water.[25,27,28]

The temperature of the sample liquid was controlled by guiding the sample tubing through a temperature bath, held at a set temperature of either 5 °C (cold) or 80 °C (warm), just before the liquid jet nozzle. It has been reported previously that the evaporative cooling rate of the liquid jet in vacuum is not well-determined for jets larger than 10 μm diameter.[17] This means the effective temperature of the liquid cannot be predicted easily. Using the (bulk) temperatures of a liquid water jet in vacuum, as reported by Wilson et al.,[17] we estimate the bulk cooling of the jet to be on the order of 15 °C between the tip of the nozzle and ionization volume, which is located $\sim$0.5 mm downstream.

Because the Auger electrons carry relatively low kinetic energy, $\sim$500 eV, the mean free path of the electrons in the liquid is $\sim$1−2 nm.[18] This means the Auger spectra contain a significant contribution from the surface layer of the liquid. Disentangling the bulk and surface contributions to the total spectrum is currently not feasible and remains a subject for future research.

■ AUTHOR INFORMATION

Corresponding Author

Olle Björneholm — *Department for Physics and Astronomy, Uppsala University, 751 20 Uppsala, Sweden;* orcid.org/0000-0002-7307-5404; Email: olle.bjorneholm@physics.uu.se

Authors

Clara-Magdalena Saak — *Department for Physics and Astronomy, Uppsala University, 751 20 Uppsala, Sweden;* orcid.org/0000-0001-7898-0713

Isaak Unger — *Department for Physics and Astronomy, Uppsala University, 751 20 Uppsala, Sweden;* orcid.org/0000-0003-1001-4134

Geethanjali Gopakumar — *Department for Physics and Astronomy, Uppsala University, 751 20 Uppsala, Sweden*

Carl Caleman — *Department for Physics and Astronomy, Uppsala University, 751 20 Uppsala, Sweden; Center for Free-Electron Laser Science, Deutsches Elektronen-Synchrotron, DE-22607 Hamburg, Germany*

Complete contact information is available at:
https://pubs.acs.org/10.1021/acs.jpclett.0c00158

REFERENCES

(1) Rye, R. R.; Madey, T. E.; Houston, J. E.; Holloway, P. H. Chemical-state effects in Auger electron spectroscopy. *J. Chem. Phys.* **1978**, *69*, 1504−1512.

(2) Öhrwall, G.; et al. The electronic structure of free water clusters probed by Augerelectron spectroscopy. *J. Chem. Phys.* **2005**, *123*, No. 054310.

(3) Lindblad, A.; Bergersen, H.; Pokapanich, W.; Tchaplyguine, M.; Öhrwall, G.; Björneholm, O. Charge delocalization dynamics of ammonia in different hydrogen bonding environments: free clusters and in liquid water solution. *Phys. Chem. Chem. Phys.* **2009**, *11*, 1758.

(4) Winter, B.; Hergenhahn, U.; Faubel, M.; Björneholm, O.; Hertel, I. V. Hydrogen bonding in liquid water probed by resonant Auger-electron spectroscopy. *J. Chem. Phys.* **2007**, *127*, No. 094501.

(5) Cederbaum, L. S.; Zobeley, J.; Tarantelli, F. Giant Intermolecular Decay and Fragmentation of Clusters. *Phys. Rev. Lett.* **1997**, *79*, 4778−4781.

(6) Jahnke, T.; et al. Ultrafast energy transfer between water molecules. *Nat. Phys.* **2010**, *6*, 139−142.

(7) Mucke, M.; Braune, M.; Barth, S.; Förstel, M.; Lischke, T.; Ulrich, V.; Arion, T.; Becker, U.; Bradshaw, A.; Hergenhahn, U. A hitherto unrecognized source of lowenergy electrons in water. *Nat. Phys.* **2010**, *6*, 143−146.

(8) Zobeley, J.; Santra, R.; Cederbaum, L. S. Electronic decay in weakly bound heteroclusters: Energy transfer versus electron transfer. *J. Chem. Phys.* **2001**, *115*, 5076−5088.

(9) Santra, R.; Zobeley, J.; Cederbaum, L. Electronic decay of valence holes in clusters and condensed matter. *Phys. Rev. B: Condens. Matter Mater. Phys.* **2001**, *64*, 245104.

(10) Thürmer, S.; Ončák, M.; Ottosson, N.; Seidel, R.; Hergenhahn, U.; Bradforth, S. E.; Slavíček, P.; Winter, B. On the nature and origin of dicationic, charge-separated species formed in liquid water on X-ray irradiation. *Nat. Chem.* **2013**, *5*, 590−596.

(11) Saak, C.-M.; Unger, I.; Brena, B.; Caleman, C.; Björneholm, O. Site-specific X-ray induced dynamics in liquid methanol. *Phys. Chem. Chem. Phys.* **2019**, *21*, 15478−15486.

(12) Nicolas, C.; Miron, C. Lifetime broadening of core-excited and -ionized states. *J. Electron Spectrosc. Relat. Phenom.* **2012**, *185*, 267−272.

(13) Hjelte, I.; Piancastelli, M.; Fink, R.; Björneholm, O.; Bässler, M.; Feifel, R.; Giertz, A.; Wang, H.; Wiesner, K.; Ausmees, A.; Miron, C.; Sorensen, S.; Svensson, S. Evidence for ultra-fast dissociation of molecular water from resonant Auger spectroscopy. *Chem. Phys. Lett.* **2001**, *334*, 151−158.

(14) Morin, P.; Miron, C. Ultrafast dissociation: An unexpected tool for probing molecular dynamics. *J. Electron Spectrosc. Relat. Phenom.* **2012**, *185*, 259−266.

(15) Richter, C.; Hollas, D.; Saak, C.-M.; Förstel, M.; Miteva, T.; Mucke, M.; Björneholm, O.; Sisourat, N.; Slavíček, P.; Hergenhahn, U. Competition between proton transfer and intermolecular Coulombic decay in water. *Nat. Commun.* **2018**, *9*, 4988.

(16) Slavíček, P.; Kryzhevoi, N. V.; Aziz, E. F.; Winter, B. Relaxation Processes in Aqueous Systems upon X-ray Ionization: Entanglement of Electronic and Nuclear Dynamics. *J. Phys. Chem. Lett.* **2016**, *7*, 234−243.

(17) Wilson, K. R.; Rude, B. S.; Smith, J.; Cappa, C.; Co, D. T.; Schaller, R. D.; Larsson, M.; Catalano, T.; Saykally, R. J. Investigation of volatile liquid surfaces by synchrotron x-ray spectroscopy of liquid microjets. *Rev. Sci. Instrum.* **2004**, *75*, 725−736.

(18) Thürmer, S.; Seidel, R.; Faubel, M.; Eberhardt, W.; Hemminger, J. C.; Bradforth, S. E.; Winter, B. Photoelectron Angular Distributions from Liquid Water: Effects of Electron Scattering. *Phys. Rev. Lett.* **2013**, *111*, 173005.

(19) Tilton, L. W.; Taylor, J. K. Accurate Representation of the Refractivity and Density of Distilled Water as a Function of Temperature. *Jounal of Research of the National Bureau of Standards* **1937**, *18*, 205−214.

(20) Narten, A. H.; Danford, M. D.; Levy, H. A. X-ray diffraction study of liquid water in the temperature range 4−200C. *Discuss. Faraday Soc.* **1967**, *43*, 97−107.

(21) Luzar, A. Extent of inter-hydrogen bond correlations in water. Temperature effect. *Chem. Phys.* **2000**, *258*, 267−276.

(22) Modig, K.; Pfrommer, B. G.; Halle, B. Temperature-Dependent Hydrogen-Bond Geometry in Liquid Water. *Phys. Rev. Lett.* **2003**, *90*, No. 075502.

(23) Seidel, R.; Pohl, M. N.; Ali, H.; Winter, B.; Aziz, E. F. Advances in liquid phase softx-ray photoemission spectroscopy: A new experimental setup at BESSY II. *Rev. Sci. Instrum.* **2017**, *88*, No. 073107.

(24) Kachel, T. The plane grating monochromator beamline U49−2 PGM-1 at BESSY II. *Journal of large-scale research facilities* **2016**, *2*, A72.

(25) Winter, B.; Weber, R.; Widdra, W.; Dittmar, M.; Faubel, M.; Hertel, I. V. Full Valence Band Photoemission from Liquid Water Using EUV Synchrotron Radiation. *J. Phys. Chem. A* **2004**, *108*, 2625−2632.

(26) Preissler, N.; Buchner, F.; Schultz, T.; Lübcke, A. Electrokinetic Charging and Evidence for Charge Evaporation in Liquid Microjets of Aqueous Salt Solution. *J. Phys. Chem. B* **2013**, *117*, 2422−2428.

(27) Kurahashi, N.; Karashima, S.; Tang, Y.; Horio, T.; Abulimiti, B.; Suzuki, Y.-I.; Ogi, Y.; Oura, M.; Suzuki, T. Photoelectron spectroscopy of aqueous solutions: Streaming potentials of NaX (X = Cl, Br, and I) solutions and electron binding energies of liquid water and X. *J. Chem. Phys.* **2014**, *140*, 174506.

(28) Olivieri, G.; Goel, A.; Kleibert, A.; Cvetko, D.; Brown, M. A. Quantitative ionization energies and work functions of aqueous solutions. *Phys. Chem. Chem. Phys.* **2016**, *18*, 29506−29515.